International Journal of Impact Engineering 120 (2018) 138–149

Contents lists available at ScienceDirect

International Journal of Impact Engineering

journal homepage: www.elsevier.com/locate/ijimpeng

Highly porous microlattices as ultrathin and efficient impact absorbers

Chang Quan Lai[a,b,*], Chiara Daraio[b]

[a] Temasek Laboratories, Nanyang Technological University, 50 Nanyang Drive 637553, Singapore
[b] California Institute of Technology, 1200 E California Blvd, Pasadena, CA 91125, USA

ARTICLE INFO

Keywords:
Auxetic
Negative Poisson's ratio
Microlattice
Impact
Shock
Bending-dominated
Stretch-dominated

The deformation and impact energy absorption properties of ultrathin polymeric microlattices were investigated as a function of density, size and positional eccentricity of the trusses, which controlled the amount of bending in the microlattice deformations. We considered highly porous, 3-D microstructures with small lattice constants (≤135 μm), and studied their response to high strain rate (~1000/s) tests, using high speed video capture, SEM imaging and quantitative modelling. The microlattices were found to have excellent impact absorption efficiencies that are 2 - 120 times better than carbon nanotube foams, polycarbonate and silicone rubber, despite being an order of magnitude slimmer than the thinnest commercial foams of similar densities. This high impact absorption efficiency is largely due to the sideways buckling of the microlattice trusses during the crushing stage, which prevented densification of the microlattices at small strains. Furthermore, we showed that varying the positional eccentricity of the trusses and the number of unit cells in the microlattices can modulate their stiffness, strength and energy absorption over an appreciable range, comparable to that obtained through modifications in relative density. Because the microlattices were mostly under stress equilibrium during the impact process, the insights derived from the present study are expected to be valid for quasistatic and low strain rate loadings as well.

1. Introduction

Shock absorbing materials are critical for the protection of portable computing devices (e.g., laptops, mobile phones and tablets) against accidental collisions and falls. Such commercial applications require protective materials to be thin (≤1 mm), both to enable rapid dissipation of the heat generated by on-chip operations and for practical packaging [1,2]. Within the electronic devices, these shock absorbers take the form of gaskets and pads placed around sensitive electronics such as hard disk drives, batteries and cameras [1,2]. Externally, they are often employed as protective cases or skins covering the entire device. As the form factor of mobile computers continue its trend towards slimmer designs, and heat management becomes more difficult with increasingly powerful computer chips and fast battery charging technology [3], there is a strong interest in developing thinner, lighter and more compact shock absorbers.

This goal, however, cannot be easily realized with current materials because of the trade-off between the minimum manufacturable thickness and the impact absorption efficiency, which is the quantity of mass/volume required to dissipate a given amount of impact energy. High porosity foams, for instance, have good impact absorption efficiencies [4–7], but because of the relatively large size and irregular arrangement of the voids within the material, they cannot be made very thin (< 1 mm) without losing uniformity in their mechanical properties (see Supplementary Information). On the other hand, low porosity foams and solid materials such as silicone rubber can be manufactured in very thin sheets (~20 μm) [8,9], but they tend to have poor impact absorption efficiencies [10–12] in the range of threshold stresses (0.1 – 10 MPa) for electronics protection [1].

To reconcile small thicknesses with high impact absorption efficiency, architected microstructures with small lattice constants (≤ 135 μm) and high porosity (> 80%) are proposed in this study. To date, experimental investigations of such ultrathin microlattices have mainly been focused on lightweight, load bearing applications, typically utilizing the stretch-dominated octet truss design [13–17], while their potential for energy absorbing applications remain largely unexplored. Therefore, the aim of this study is to characterize the mechanical properties and deformation of the microlattices under dynamic loading conditions, and assess their viability as slim and efficient impact absorbers.

* Corresponding author at: Temasek Laboratories, Nanyang Technological University, 50 Nanyang Drive 637553, Singapore.
E-mail address: cqlai@ntu.edu.sg (C.Q. Lai).

https://doi.org/10.1016/j.ijimpeng.2018.05.014
Received 20 December 2017; Received in revised form 4 May 2018; Accepted 30 May 2018
Available online 20 June 2018
0734-743X/

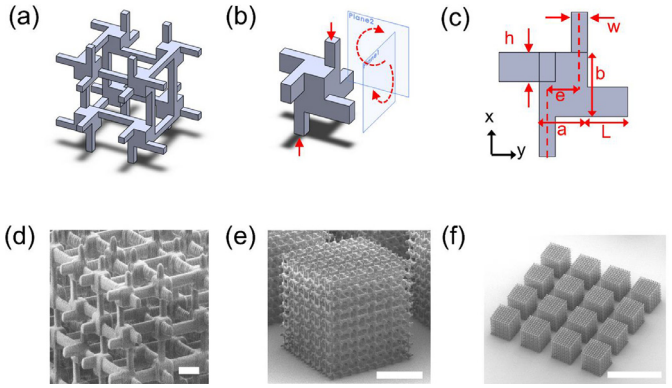

Fig.1. Schematic diagram of (a) a unit cell (b) a sub-unit cell in isometric view and (c) a sub-unit cell in 2 dimensions. SEM images of (d) close-up view of the fabricated unit cells (Scale bar is 10 μm), (e) a single microlattice (Scale bar is 100 μm), (f) a 4 × 4 array of microlattices on a single test sample (Scale bar is 500 μm).

2. Materials and methods

2.1. Microlattice design and fabrication

A unit cell in the microlattice (Fig. 1a) was composed of 8 subunits, each adjacently linked to their mirror images. The subunit (Fig. 1b) consisted of 6 trusses attached to a central cuboid which had dimensions, *a* (length) x *a* (width) x *b* (height) (Fig. 1c). The dimensions of the vertical trusses were *L* (length) x *w* (width) x *w* (height), while that of the horizontal trusses were *L* (length) x *w* (width) x *h* (height) (Fig. 1c). The subunit cells were then assembled into microlattices (Fig. 1d and e). In most experiments, multiple microlattices were placed on a single sample (Fig. 1e) to ensure that the compressive force would be sufficiently large for detection by the piezoelectric sensors during impact testing.

The microlattice geometry described above was chosen because bending deformations of the individual truss elements can be varied systematically using a single geometric parameter, *e*. This facilitated the analysis of the mechanical response of microlattices with respect to the underlying deformation mechanisms (Fig. 1c). For $e = 0$ μm, the lattice design was essentially simple cubic, and its uniaxial deformation was compression-dominated (i.e., stretch-dominated; see Supplementary Information). For $e > 0$ μm, a uniaxial load generated a rotation of the central cuboid, causing the trusses to bend (Fig. 1b). With increasing *e*, the bending moment for a given load increased, and therefore, the lattice deformation transitioned from one that was stretch-dominated to one that was bending-dominated. In addition, it can be seen that bending of the horizontal trusses under uniaxial compressive loading would pull the sub-unit cells closer together, shortening the overall width of the microlattice. Therefore, microlattices with $e > 0$ were expected to have a negative Poisson's ratio. Auxetic designs that work on a similar principle had previously been studied in 2-D as well [18,19].

Other than the effect of buckling due to eccentricity (Fig. 2a), we also studied the effects of relative density, by varying the length of the trusses, *L* (Fig. 2b), and of the relative lattice size, by varying the number of subunit cells, *n*, along the length of the lattice (Fig. 2c). The relative density, *r*, refers to the ratio of the lattice density to that of the constituent material, and it is quantitatively equivalent to (1 - porosity). The relative lattice size is determined with respect to the length of the subunit cell, following the convention established in previous studies of stochastic foams, which traditionally characterized the width of gaps in the foams as the cell length [20,21]. The full geometrical details of the fabricated microlattices, measured using SEM images, are given in Table 1.

To fabricate the microlattices, STL files of the models, such as those shown in Fig. 1a–c, were first transferred into a commercial instrument, Photonics Professional GT (Nanoscribe GmbH). Based on the information of these files, the equipment then employed a galvo-mirror system to mechanically position the focal point of an infrared laser at various points within a liquid negative photoresist, IP-Dip (Nanoscribe GmbH), which was deposited on a 2.5 cm × 2.5 cm glass slide. The sections of the negative photoresist that were exposed to this laser focal point then solidified due to 2-photon polymerization, forming the microlattice structures shown in Figs. 1d–f and 2. Unpolymerized photoresist resin was removed through 10 min of isopropyl alcohol immersion, after which the samples were allowed to dry in ambient. The density of cured IP-Dip is 1300 kg/m^3 [13] and the strain-rate dependence of its Young's modulus, *E*, and yield stress, σ_y, were characterized and reported in the Supplementary Information. For the parameters in this study, *E* and σ_y were found to be approximately 1.35 ± 0.03 GPa and 76.5 ± 6.5 MPa respectively, which are similar to the quasistatic values reported previously [16].

2.2. Dynamic testing

We performed impact tests on the microlattices using a custom, horizontal impact test setup (Fig. 3) [22–24]. In this system, the microlattices were impacted by a striker that, upon pneumatic activation, slid through a 200 mm long frictionless channel built with air bearings (Newway®). The striker in our tests was made from Delrin polymer ($E = 3.1$ GPa, mass = 10.22 g). The samples were mounted on top of a piezoelectric element (model 200B03, PCB Piezotronics Quartz ICP). The velocity of the striker varied between 0.15 m/s and 0.25 m/s (strain rate = 600/s–1000/s) at the onset of impact.

The striker was fitted with Moire's gratings (pitch = 25 μm) and as it neared the samples, a separate, stationary Moire's gratings on top of the channel created an interference pattern [22–24]. By tracking the intensity of a laser light focused on this interference pattern through an oscilloscope (Tektronix DPO 3034), the distance-time plot of the striker can be obtained. Together with the force-time plot provided by the piezoelectric element which was connected to the same oscilloscope (sampling rate = 10^7/s), the force-distance plot, and consequently, the stress-strain plot for each impact experiment was computed. Because of the small thickness of the samples, the microlattices reached dynamic stress equilibrium very quickly (the ringing-up time was estimated at ~ 0.2% of the impact duration [5]) and thus, even the elastic, small deformation regime of the impact process could be reliably examined.

Each impact test was also recorded with a high-speed camera, Phantom V12.1 (Vision Research), operated at 8000 fps, exposure time of 105 μs and resolution of 1024 pixels × 768 pixels. The camera was fitted with K2/SC long distance magnifying lenses (Infinity Photo-optical Co.), with a resolution of 2 μm/pixel.

2.3. SEM microscopy

Pristine microlattices and microlattices that were crushed after dynamic testing, were characterized using a Hitachi Nanoshield scanning electron microscope (SEM) at 1 kV. The microlattices were sputtered with a 5 nm thick Pt layer prior to SEM examination, to improve the image quality at high resolution scanning. Due to the Pt coating, pristine microlattices subjected to SEM examination were not used for experimental testing.

3. Results

The raw (light blue) and filtered (dark blue) dynamic stress-strain plots obtained from impact tests on microlattices with varying *e, r* and *n* are presented in Fig. 4, Fig. 5 and Fig. 6 respectively. It can be observed that each plot can generally be separated into 4 distinct regimes as indicated in the schematic diagram in Fig. 7a. In stage A, the initial